Transcriptome analysis after PPARγ activation in human meibomian gland epithelial cells (hMGEC)

Sun Woong Kim[a,b], **Donald J. Brown[b]**, **James V. Jester[b,*]**

[a]Department of Ophthalmology, Yonsei University Wonju College of Medicine, Wonju, South Korea

[b]Gavin Herbert Eye Institute, University of California, Irvine, CA, United States

Abstract

Purpose—PPARγ plays a critical role in the maturation of immortalized human meibomian gland epithelial cells (hMGEC). To further understand the molecular changes associated with meibocyte differentiation, we analyzed transcriptome profiles from hMGEC after PPARγ activation.

Methods—Three sets of cultivated hMGEC with or without exposure to PPARγ agonist, rosiglitazone were used for RNA-seq analysis. RNA was isolated and processed to generate 6 libraries. The libraries were then sequenced and mapped to the human reference genome, and the expression results were gathered as reads per length of transcript in kilobases per million mapped reads (RPKM) values. Differential gene expression analyses were performed using DESeq2 and NOISeq. Gene ontology enrichment analysis (GOEA) was performed on gene sets that were upregulated or downregulated after rosiglitazone treatment. Five genes were selected for validation and differential expression was confirmed using quantitative PCR. The Differential expression of CK5 was evaluated using Western blotting.

Results—Expression data indicated that about 58,000 genes are expressed in hMGEC. DESeq2 and NOISeq indicated that 296 and 3436 genes were upregulated and 258 and 3592 genes were down regulated after rosiglitazone treatment, respectively. Of genes showing significant differences >2 fold, GOEA indicated that cellular and metabolic processes were highly represented. Expression of *ANGPTL4, PLIN2, SQSTM1*, and *DDIT3* were significantly upregulated and *HHIP* was downregulated by rosiglitazone. CK5 was downregulated by rosiglitazone.

Conclusions—The RNA-seq data suggested that PPARγ activation induced alterations in cell differentiation and metabolic process and affected multiple signaling pathways such as PPAR, autophagy, WNT, and Hedgehog.

*Corresponding author. 843 Health Sciences Road, University of California, Irvine, CA, 92697-4390, United States., JJester@uci.edu (J.V. Jester).

1. Introduction

The peroxisome proliferator activator receptor, PPARγ is a ligand-activated transcription factor, which is actively involved in the regulation of metabolism of lipid, glucose homeostasis, cell proliferation, and cell differentiation. Being modulated by variety of ligands, PPARγ is considered as a crucial metabolic sensor modulating numerous gene expression programs implicated in homeostasis. One of the major challenges that remain is to better understand molecular mechanism underlying PPARγ′s tissue and ligand specific activity [1–3]. Previous studies have shown that PPARs play an important role in sebocyte differentiation [4–7]. However, the exact role that specific PPAR ligands and receptors play on holocrine exocrine gland differentiation and lipid production remain unclear. Studies carried out in rat preputial cells indicate that PPAR ligands such as fibrates, linoleic acid, and thiazolidinediones increase lipid droplets [4,5]. Studies carried out in SZ95 sebocytes indicate that linoleic acid, but not other ligands of PPAR-α or -γ, increase lipid production [5–7]. However, studies in isolated human sebaceous gland indicate that linoleic acid decrease lipogenesis [8]. From the metabolic point of view, PPAR-α and δ are mainly involved in catabolic processes, whereas PPARγ regulates anabolic lipid biosynthesis, and other PPAR isotypes show different tissue specific activities [9].

Our group has hypothesized PPARγ is a crucial regulator of meibocyte differentiation and have shown that PPARγ agonist, rosiglitazone, triggers differentiation and lipogenesis in cultured mouse meibocytes as well as in immortalized human meibomian gland epithelial cells (hMGEC) [10,11]. Downregulation of PPARγ has been associated with gland atrophy in aged mice and human meibomian glands [12–14]. In vitro studies demonstrated that meibocyte differentiation was suppressed by blocking PPARγ signaling using a specific PPARγ antagonist in hMGEC. We have also documented that the PPARγ agonist rosiglitazone induced cell cycle exit and meibocyte differentiation [12–14]. Taking into consideration of tissue specific role of PPARγ in the induction of meibocyte differentiation has prompted us to identify the effect of PPARγ activation on gene expression in hMGECs.

Transcriptome analysis by RNA-seq has become more popular for differential expression analysis involving specific conditions. The correct identification of differentially expressed genes (DEGs) between specific conditions is key to understanding phenotypic variation [15,16]. In this context, identification of gene expression changes after activating PPARγ signaling would be valuable to elucidating the molecular mechanisms controlling meibocyte differentiation. Here we conducted RNA-seq to identify DEGs in hMGECs exposed to rosiglitazone. Gene ontology (GO) analysis revealed that genes associated with cellular differentiation and metabolic processes were significantly altered after rosiglitazone treatment.

2. Materials and methods

2.1. Cultivation and differentiation of hMGEC

Immortalized hMGEC, a generous gift from Dr. Sullivan (Schepens Eye Research Institute), was grown in KSFM media (Invitrogen-Gibco, Grand Island, NY) as previously described [17]. At 80% confluency, differentiation was induced by culturing cells in DMEM-F12 (Gibco, Grand Island, NY) supplemented with Epidermal Growth Factor (EGF, 10 ng/ml, Sigma) with or without adding the PPARγ agonist, rosiglitazone (30 μM, Sigma, St. Louis, MO). Culture media was changed every other day and differentiation conditions were maintained for 1–6 days depending on analysis.

2.2. RNA isolation and library construction

Three independent paired cultures of hMGECs with or without exposure to rosiglitazone were used for RNA seq analysis. Two pairs were exposed for 24 h (set1 and 2) and 1 pair (set 3) was exposed for 48 h. RNA was isolated using the RNeasy Mini kit following the manufacturer's instructions (Qiagen, Valencia, CA). Library construction and sequencing were conducted in the Genomics High Throughput Facility at UCI. RNA quality and quantity was assessed with the aid of an Agilent 2100 Bioanalyzer (Agilent Technologies, Santa Clara, CA) and ribosome integrity number (RIN) was evaluated for each sample (scaled from 1 to 10, with 10 the maximum value). All samples had a RIN of 10. Poly A+ containing RNA was enriched from 1 μg of total RNA using poly dT magnetic beads. The enriched fraction was chemically fragmented using a TruSeq RNA Sample Prep kit v2 (Illumina, San Diego, CA). This resulted in a non-stranded library for each RNA pool with distinct bar code adapters to discriminate the source (3 controls vs. 3 rosiglitazone treated). The libraries were then sequenced on an Illumina HiSeq 4000 within a single column to generate approximately 50 million reads (single read sequencing 100 cycles) from each library.

2.3. RNA-seq data analysis

The raw FASTQ sequence files were uploaded in a cloud computing platform launched by Sequentia Biotech (Barcelona, Spain), A.I.R. (Artificial intelligence RNA-Seq, https://transcriptomics.sequentiabiotech.com). The A.I.R. is RNA-Seq data analysis platform capable of automatically analyzing and comparing RNA samples and interpreting data in the same program. Uploaded FASTQ files undergo quality assessment and filtering in the program. Sequences trimmed of adapter were mapped to the human reference genome (GRCh38). Expression results were gathered as RPKM (number of mapped Reads Per length of transcript in Kilobases per Million mapped reads) values for each gene. All these analytical processes were automatically performed and provided by A.I.R. Based on RPKM values, genes were divided into four expression categories: very low or not expressed, low, medium or highly expression. Briefly, genes with an average RPKM value across samples below 0.125 were considered to be very low or not expressed, genes with an average RPKM value between 0.125 and 1 were considered low expression, between 1 and 10 medium expression, and above 10 to be highly expressed [18]. The A.I.R. platform provides 4 bioinformatics algorithms (DESeq2, edgeR, EBSeq, and NOISeq) for differential gene expression analyses. Since there is no consensus regarding which method has the best

performance, we used Deseq2 and NOISeq software to generate DEGs and GO analysis. The DESeq2 package provides methods to test for differential expression by use of negative binomial generalized linear models. It is one of the leading methods of analysis due to its high sensitivity and low false discovery rate. The NOISeq is a non-parametric approach for the identification of differentially expressed genes from data. It gives higher false positives with respect to the aforementioned method, however it is particularly suited for experiments where high variability is observed across the replicates, as it is able to identify more differentially expressed genes compared to DESeq2 in these conditions. It is also known to be suitable for experiments with small number of replicates [15,16]. Since our samples showed relatively high variability between replicates, and we used only 3 replicates per group, a non-parametric approach, NOISeq was chosen for analysis. However, to reduce high false positives with respect to NOISeq, DEGs were restricted to transcripts showing expression greater than 2 fold changes and P-value   0.01. We also present the result of DESeq2 for comparison. The complete lists of DEGs are available in S1–4 tables. Further gene ontology analysis and pathway analysis were done using PANTHER (http://www.pantherdb.org/).

2.4. Differential expression of selected genes

Among identified DEGs, genes suggested to be differentially expressed in both algorithms were reviewed and 5 genes were selected for further validation. mRNA expression of 5 genes (*PLIN2*, perilipin 2; *ANGPTL4*, angiopoietin like 4; *SQSTM1*, sequestosome 1; *DDIT3*, DNA damage inducible transcript 3; and *HHIP*, hedgehog interacting protein) were evaluated using the quantitative real time PCR as described previously [10]. Briefly, 1 μg of RNA was reverse transcribed using oligo dT and random primers as supplied in the QuantiTect Reverse Transcription Kit (Qiagen). Real time PCR was performed using FastStart Essential DNA green master (Roche, Indianapolis, IN) with Lightcycler 96 system (Roche) and predesigned SYBR green real time PCR primers (http://www/sigmaaldrich/catalog/product/sigma/kspq12012). Relative quantization was performed using the delta CT method using GAPDH as the normalizing housekeeper gene.

2.5. Protein extraction and western blotting

Cells were lysed on ice using the Pro-prep™ protein extraction kit (Intron Biotechnology, Korea), and western blot analysis was performed as described previously [5]. Briefly, 20 μg of protein lysates was resolved by 10% Mini-PROTEAN TGX gels (Bio-Rad, Hercules, CA) and transferred to a PVDF membrane (Invitrogen). The membrane was blocked for 1 h in PBS containing 5% skim milk and 0.2% Tween-20 and incubated overnight with primary antibodies for Cytokeratin 5 (CK5, Abcam, Cambridge, MA, ab53121, 1:1000 dilution). Antibody-reactive proteins were detected by means of the appropriate HRP-conjugated secondary antibodies and an enhanced chemiluminescent substrate (SuperSignal™ West Pico Chemiluminescent Substrate, Thermo scientific). Immunostained bands were imaged and analyzed with ChemiDoc MP (Bio-Rad) and relative quantitation was done after normalization to GAPDH band in same blots.

3. Results

3.1. Rosiglitazone induced differential gene expression related to multiple cellular and metabolic processes

Sequencing quality was overall good with no sequences flagged with bad. BAM (binary alignment map) quality revealed a sample flagged with bad quality because the number of reads assigned to genes was relatively low (74.6%) in one sample treated with rosiglitazone (rosi1 in set1). Before statistical comparison for differential expression, we assessed the variation of data using principal component analysis (PCA) clustering plot provided by A.I.R. It showed an outlier, the same sample flagged with bad quality in BAM (rosi1 in set1) and this was removed from further analysis (Fig. 1A). Fig. 1B shows the PCA plot for the control and rosiglitazone treatment groups after excluding 1 outlier. According to PCA, the major variation of gene expressions occurred due to culture period, which was separated by PC1 (set1 and 2: 1 day differentiation vs. set 3: 2 day differentiation). To investigate the effect of activating PPARγ by rosiglitazone, we compared DEGs between cluster of control and rosiglitazone treatment in the current study.

A total 15,743 genes were identified with RPKM values greater than or equal to 0.125 and 4026 genes were considered to be highly expressed with RPKM over 10. Not unexpected for epithelial origin, multiple keratin genes were all highly represented in these libraries. The DESeq2 identified about 58233 genes and 554 were differentially expressed (296 up and 258 down). Among them, 67 genes were upregulated and 87 genes were downregulated with more than a 2 fold change in cells treated with rosiglitazone as compared to cells cultured with DMEM/F12 and EGF alone. Fig. 2 shows expression patterns of the differentially expressed genes (DEG) in a heat map. Changes in expression levels are displayed from green (less expressed) to red (more expressed). Overall, a quite different pattern of gene expression was observed between control and rosiglitazone treatment group. It also showed similarity within 1d sets (set1 vs. 2) and difference between 1d and 2d of differentiation (set1, 2 vs. 3) within each experimental group. The NOISeq, which is a non-parametric method useful for relatively small number of replicates, identified 3436 upregulated and 3591 down regulated genes. Among them, 219 genes were upregulated and 360 genes were down-regulated more than 2 folds with FDR 0.01. Of note, these genes were all identified in DESeq2. Fig. 3 shows volcano plot from DESeq2 analysis with name of some genes ranked high based on fold change and statistical significance. From these data sets, using a further restriction requiring more than 2 fold change by both DESeq2 and NOIseq, 67 genes were upregulated and 87 genes were downregulated in cells treated with rosiglitazone as compared to cells differentiated under DMEM/F12 with EGF.

Gene ontology enrichment analysis (GOEA) of these genes emphasized that the biologic processes most affected by rosiglitazone was in those pathways involving cellular and metabolic processes. As shown in Fig. 4A, evaluating those genes overexpressed in cells exposed to rosiglitazone, two pathways were prominently enriched and highly represented by genes involved with cell communication, cell cycle, lipid metabolic process and biosynthetic process. Evaluating genes downregulated in cells exposed to rosiglitazone, cellular process and metabolic process also were primarily affected (Fig. 4B). Tables 1 and 2

summarized GOEA results showing some ontology annotations containing 5 genes, FDR < 0.01, and enrichment score > 2 using DESeq2. Interestingly, these data indicated that cell differentiation, response to stimulus, cell signaling, cell cycle and other various regulation pathways are highly represented, suggesting that rosiglitazone induced alterations in multiple processes.

3.2. Rosiglitazone induced upregulation of ANGPTL4, PLIN2, SQSTM 1, DDIT3 and downregulation of HHIP

Full lists of upregulated and downregulated genes by rosiglitazone are Supplemental Tables 1–4. Table 3 shows selected sets of DEGs after rosiglitazone treatment. Rosiglitazone induced upregulation of various genes related to lipid biosynthesis or transport such as *ANGPTL4, PLIN2, CD36, CEBPA, ELOVL4,* and *ELOVL7*. Furthermore, as shown in GO analysis, many genes related to cell cycle (*CCNE2, PCNA*), autophagy (*ATG9B, SQSTM1*), differentiation (*CK5*), and cell to cell signaling (*IRS2, SQSTM1, DDIT3,* and *HHIP*) were differentially expressed. Among those identified, we selected five genes for validation, which are related to lipid synthesis or meibocyte differentiation (*PLIN2* and *ANGPTL4*), cell cycle and WNT signaling (*DDIT3*), autophagy and NF-kB signaling (*SQSTM1*), and hedgehog signaling (HHIP). As shown in Fig. 5A, rosiglitazone increased expression of *ANGPTL4, PLIN2, SQSTM 1,* and *DDIT3* by 3.4, 3.2, 2.6, and 2.2 folds, respectively. By contrast, *HHIP* was downregulated after treatment with rosiglitazone by 2.2 fold. Upregulation of *ANGPTL4, PLIN2,* and *SQSTM1* were maintained to 6 days of differentiation (Fig. 5B).

3.3. Rosiglitazone downregulated expression of cytokeratin 5

RNA seq data shows that multiple keratin genes were highly expressed in hMGEC, as expected in epithelial cell origin. Since keratin expression has been studied with regard to epithelial differentiation, we searched for whether rosiglitazone affected expression of meibocyte specific keratins. DESeq2 identified *CK5* was decreased after rosiglitazone treatment by 1.7 fold and *CK1*4 by 1.4 from our RNA seq data. Fig. 6 confirmed that the protein expression of CK5 decreased after rosiglitazone treatment.

4. Discussion

Using RNA-seq, we quantified gene expression in hMGEC in the presence or absence of rosiglitazone. Our study focused on role of PPARγ and we chose rosiglitazone as it is known to have a selective PPARγ specificity. This approach enabled us to investigate the effects of activation of PPARγ signaling in hMGECs. In agreement with our previous reports [10,11], rosiglitazone altered the expression of genes related to cell cycle, differentiation, and lipid metabolic pathways. Cellular and metabolic processes are the two most enriched biological processes and multiple genes related to cell cycle, signal transduction, lipid synthesis and metabolism were altered after rosiglitazone treatment. Our recent work showed that PPARγ signaling induces cell cycle exit as well as meibocyte differentiation indicated by the accumulation of neutral lipids and lipogenic gene expression [10,11]. Of interest, the most enriched GO entities of down-regulated genes were those in the initiation of DNA replication and G1/S cell cycle transition, supporting our earlier

finding that rosiglitazone induced cell cycle exit. With regard to meibocyte differentiation, rosiglitazone upregulated multiple genes related to lipid synthesis or transport such as *ANGPTL4, PLIN2, CD36, CEBPA, ELOVL4*, and *ELOVL7* (Table 3). If we expanded our search for differential gene expression to include genes with less than 2 fold changes, many more genes involved with lipid synthesis were identified as being upregulated. Of particular note, rosiglitazone induced alterations in gene expression related to various signaling pathways such as FGF, Insulin/IGF, PI3 kinase, MAPK, Notch, WNT, Hedgehog, and so on. Although it is not clear whether these alterations are directly related to PPARγ activation, at least, it can be concluded that there must be a complex and orchestrated network of signaling pathways directly or indirectly associated with PPARγ activation during differentiation of this cell line.

Among various DEGs, we selected some genes, which are presumed to be related to the meibocyte differentiation pathway. First, *ANGPTL4* was one of the most highly induced genes after rosiglitazone treatment. The encoded protein is known to be induced by peroxisome proliferation activators and functions as a hormone that regulates glucose homeostasis, lipid metabolism, and insulin sensitivity. Its expression is strongly induced during adipocyte as well as sebocyte differentiation [19–21], supporting it's up-regulation during meibocyte differentiation. Secondly, *PLIN2* encodes a protein that is associated with surface membrane of lipid droplet, and has been shown to be involved in the development and maintenance of adipose tissue. It is also known to serve as a marker of lipid accumulation [22,23]. We have already reported that rosiglitazone upregulated expression of *PLIN2* significantly after 2d of treatment with rosiglitazone in a previous report [11], and reconfirmed this in hMGECs exposed to rosiglitazone for 1d. Thirdly, *SQSTM1* encodes a multifunctional protein that binds ubiquitin and regulates activation of the nuclear factor kappa-B (NF-kB) signaling pathway. It also functions as a bridge between ubiquitinated cargo and autophagosomes. The intracellular level of p62/SQSTM1 is regulated by a fine balance between transcriptional regulation and post-translational autophagic degradation [24,25]. It has not been reported yet that SQSTM1 is regulated by rosiglitazone, and further studies are needed to identify whether the upregulation of SQSTM1 is associated with induction of autophagy during meibocyte differentiation. Fourthly, *DDIT3* gene encodes multifunctional transcription factor in ER stress response. It plays an essential role in the response to a wide variety of cell stresses and induces cell cycle arrest and apoptosis in response to ER stress. It inhibits the canonical Wnt signaling pathway by binding to TCF7L2/TCF4, impairing its DNA-binding properties and repressing its transcriptional activity [26]. Lastly, *HHIP* gene encodes a member of the hedgehog-interacting protein (HHIP) family. The hedgehog (HH) proteins are evolutionarily conserved protein, which are important morphogens for a wide range of developmental processes, including anteroposterior patterning of limbs and regulation of left-right asymmetry in embryonic development. Multiple cell-surface receptors are responsible for transducing and/or regulating HH signals. The HHIP encoded by this gene is a highly conserved, vertebrate-specific inhibitor of HH signaling [27]. These data reconfirmed that rosiglitazone induced alterations in genes related to meibocyte differentiation as well as multiple signaling cascades including autophagy, Wnt, and Hedgehog signaling.

Although differential expression levels were less than 2 fold, we further investigated effect of rosiglitazone on expression of cytokeratins (CK). While the basal acinar cell of the meibomian glands only express CK5, the meibomian gland duct shows expression of CK5, CK6 and CK 14 [28]. Previous studies reported that serum induced hyperkeratinization by showing upregulation of various CKs [29]. Of note, rosiglitazone decreased expression of CK5 and CK14 in our RNA-seq data. We performed WB for CK5 and confirmed that rosiglitazone decreased expression of CK5. Given that CK5 is only expressed at the basal layer, this result suggests that rosiglitazone triggers differentiation in culture.

Our RNA-Seq data also revealed some potential limitations to using hMGEC. We noticed that some gene expression profiles are different than previous reports. For example, AWAT1 and 2 (Acyl-CoA wax alcohol acyltransferase) expression were not detected in control cells and FAR2 was expressed at low levels. Furthermore, expressions of these enzymes were not induced by rosiglitazone treatment. These enzymes have been known to be highly expressed in both human and mice tarsal plate [30,31]. Given that they play key roles in producing elongated chain fatty alcohols and wax esters (WE), this difference in gene expression pattern may explain the inability of identifying meibum specific lipids using lipidomic analysis of differentiated hMGEC. Also, this indicates the possibility of other important signaling cascades being involved with upregulation of these enzymes and meibocyte differentiation.

It also should be noted that different ligands induce different effects via PPARγ and/or other PPAR signaling pathways. Specifically, natural ligands such as various fatty acids and lipids could activate not only PPARγ but also other isoforms [9,32]. Trivedi et al. reported that rosiglitazone increased lipid production in sebocytes, whereas another PPARγ ligand pioglitazone did not [6]. Previous work has also shown that rosiglitazone induced cholesterol and TG synthesis in sebocytes, whereas arachidonic acid did not increase cholesterol levels but rather caused remodeling of lipid species bearing fatty acid side chains [21]. The discrepancy can be attributed to specific modifications of tridimensional conformation of the receptor induced by various ligands that lead to different transcriptional activities of PPARs or due to the tissue specificity. Taken together, the observed responses reported in this paper should be ascribed specifically to the activation of PPARγ by rosiglitazone and not necessarily representative of other PPAR ligands, which may produce similar or different effects.

5. Conclusion

This study shows that rosiglitazone induces alterations in cell cycle, signaling, and lipid metabolism at least partly by activating PPARγ. Cross talk between PPARγ and other signaling cascades need to be clarified to more fully understand meibocyte differentiation.

Supplementary Material

Refer to Web version on PubMed Central for supplementary material.

Acknowledgments

## References

[1]. Janani C, Ranjitha Kumari BD. PPAR gamma gene-a review. Diabetes, Metab Syndrome 2015;9:46–50.

[2]. Li Y, Jin D, Xie W, Wen L, Chen W, Xu J, et al. PPAR-gamma and Wnt regulate the differentiation of MSCs into adipocytes and osteoblasts respectively. Curr Stem Cell Res Ther 2018;13:185–92. [PubMed: 29034841]

[3]. Takada I, Kouzmenko AP, Kato S. PPAR-gamma signaling crosstalk in mesenchymal stem cells. PPAR Res 2010;2010.

[4]. Rosenfield RL, Deplewski D, Kentsis A, Ciletti N. Mechanisms of androgen induction of sebocyte differentiation. Dermatology 1998;196:43–6. [PubMed: 9557223]

[5]. Chen W, Yang CC, Sheu HM, Seltmann H, Zouboulis CC. Expression of peroxisome proliferator-activated receptor and CCAAT/enhancer binding protein transcription factors in cultured human sebocytes. J Invest Dermatol 2003;121:441–7. [PubMed: 12925198]

[6]. Trivedi NR, Cong Z, Nelson AM, Albert AJ, Rosamilia LL, Sivarajah S, et al. Peroxisome proliferator-activated receptors increase human sebum production. J Invest Dermatol 2006;126:2002–9. [PubMed: 16675962]

[7]. Makrantonaki E, Zouboulis CC. Testosterone metabolism to 5 alpha-dihydrotestosterone and synthesis of sebaceous lipids is regulated by the peroxisome proliferator-activated receptor ligand linoleic acid in human sebocytes. Br J Dermatol 2007;156:428–32. [PubMed: 17300229]

[8]. Downie MM, Sanders DA, Maier LM, Stock DM, Kealey T. Peroxisome proliferator-activated receptor and farnesoid X receptor ligands differentially regulate sebaceous differentiation in human sebaceous gland organ cultures in vitro. Br J Dermatol 2004;151:766–75. [PubMed: 15491415]

[9]. Wang L, Waltenberger B, Pferschy-Wenzig EM, Blunder M, Liu X, Malainer C, et al. Natural product agonists of peroxisome proliferator-activated receptor gamma (PPARgamma): a review. Biochem Pharmacol 2014;92:73–89. [PubMed: 25083916]

[10]. Jester JV, Potma E, Brown DJ. PPARgamma regulates mouse meibocyte differentiation and lipid synthesis. Ocul Surf 2016;14:484–94. [PubMed: 27531629]

[11]. Kim SW, Xie Y, Nguyen PQ, Bui VT, Huynh K, Kang JS, et al. PPARgamma regulates meibocyte differentiation and lipid synthesis of cultured human meibomian gland epithelial cells (hMGEC). Ocul Surf 2018;16:463–9. [PubMed: 29990545]

[12]. Nien CJ, Massei S, Lin G, Nabavi C, Tao J, Brown DJ, et al. Effects of age and dysfunction on human meibomian glands. Arch Ophthalmol 2011;129:462–9. [PubMed: 21482872]

[13]. Nien CJ, Paugh JR, Massei S, Wahlert AJ, Kao WW, Jester JV. Age-related changes in the meibomian gland. Exp Eye Res 2009;89:1021–7. [PubMed: 19733559]

[14]. Jester JV, Brown DJ. Wakayama Symposium: peroxisome proliferator-activated receptor-gamma (PPARgamma) and meibomian gland dysfunction. Ocul Surf 2012;10:224–9. [PubMed: 23084144]

[15]. Seyednasrollah F, Laiho A, Elo LL. Comparison of software packages for detecting differential expression in RNA-seq studies. Briefings Bioinf 2015;16:59–70.

[16]. Costa-Silva J, Domingues D, Lopes FM. RNA-Seq differential expression analysis: an extended review and a software tool. PLoS One 2017;12:e0190152. [PubMed: 29267363]

[17]. Liu S, Hatton MP, Khandelwal P, Sullivan DA. Culture, immortalization, and characterization of human meibomian gland epithelial cells. Invest Ophthalmol Vis Sci 2010;51:3993–4005. [PubMed: 20335607]

[18]. Hackett NR, Butler MW, Shaykhiev R, Salit J, Omberg L, Rodriguez-Flores JL, et al. RNA-Seq quantification of the human small airway epithelium transcriptome. BMC Genomics 2012;13:82. [PubMed: 22375630]

[19]. Zhu S, Cheng G, Zhu H, Guan G. A study of genes involved in adipocyte differentiation. J Pediatr Endocrinol Metab 2015;28:93–9. [PubMed: 25153216]

[20]. Dahlhoff M, Camera E, Picardo M, Zouboulis CC, Schneider MR. Angiopoietin-like 4, a protein strongly induced during sebocyte differentiation, regulates sebaceous lipogenesis but is dispensable for sebaceous gland function in vivo. J Dermatol Sci 2014;75:148–50. [PubMed: 24815769]

[21]. Dozsa A, Dezso B, Toth BI, Bacsi A, Poliska S, Camera E, et al. PPARgamma-mediated and arachidonic acid-dependent signaling is involved in differentiation and lipid production of human sebocytes. J Invest Dermatol 2014;134:910–20. [PubMed: 24129064]

[22]. Dahlhoff M, Camera E, Picardo M, Zouboulis CC, Chan L, Chang BH, et al. PLIN2, the major perilipin regulated during sebocyte differentiation, controls sebaceous lipid accumulation in vitro and sebaceous gland size in vivo. Biochim Biophys Acta 2013;1830:4642–9. [PubMed: 23688400]

[23]. Takahashi Y, Shinoda A, Kamada H, Shimizu M, Inoue J, Sato R. Perilipin 2 plays a positive role in adipocytes during lipolysis by escaping proteasomal degradation. Sci Rep 2016;6:20975. [PubMed: 26876687]

[24]. Shi J, Wong J, Piesik P, Fung G, Zhang J, Jagdeo J, et al. Cleavage of sequestosome 1/p62 by an enteroviral protease results in disrupted selective autophagy and impaired NFKB signaling. Autophagy 2013;9:1591–603. [PubMed: 23989536]

[25]. Chang CP, Su YC, Lee PH, Lei HY. Targeting NFKB by autophagy to polarize hepatoma-associated macrophage differentiation. Autophagy 2013;9:619–21. [PubMed: 23360732]

[26]. Horndasch M, Lienkamp S, Springer E, Schmitt A, Pavenstadt H, Walz G, et al. The C/EBP homologous protein CHOP (GADD153) is an inhibitor of Wnt/TCF signals. Oncogene 2006;25:3397–407. [PubMed: 16434966]

[27]. Vidal MT, Lourenco SV, Soares FA, Gurgel CA, Studart EJ, Valverde Lde F, et al. The sonic hedgehog signaling pathway contributes to the development of salivary gland neoplasms regardless of perineural infiltration. Tumour Biol 2016;37:9587–601. [PubMed: 26790448]

[28]. Hwang HS, Parfitt GJ, Brown DJ, Jester JV. Meibocyte differentiation and renewal: insights into novel mechanisms of meibomian gland dysfunction (MGD). Exp Eye Res 2017;163:37–45. [PubMed: 28219733]

[29]. Hampel U, Schroder A, Mitchell T, Brown S, Snikeris P, Garreis F, et al. Seruminduced keratinization processes in an immortalized human meibomian gland epithelial cell line. PLoS One 2015;10:e0128096. [PubMed: 26042605]

[30]. Parfitt GJ, Brown DJ, Jester JV. Transcriptome analysis of aging mouse meibomian glands. Mol Vis 2016;22:518–27. [PubMed: 27279727]

[31]. Butovich IA. Meibomian glands, meibum, and meibogenesis. Exp Eye Res 2017;163:2–16. [PubMed: 28669846]

[32]. Echeverria F, Ortiz M, Valenzuela R, Videla LA. Long-chain polyunsaturated fatty acids regulation of PPARs, signaling: relationship to tissue development and aging. Prostaglandins Leukot Essent Fatty Acids 2016;114:28–34. [PubMed: 27926461]
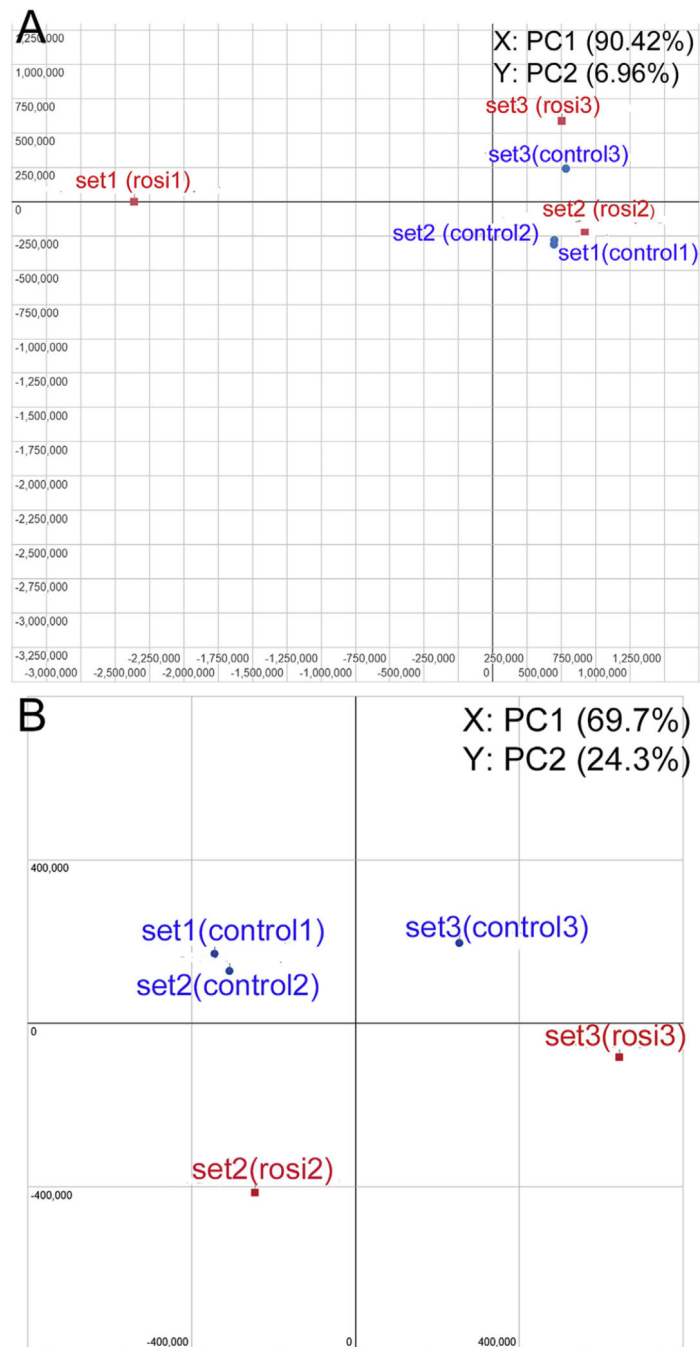
Fig. 1.
PCA (principal component analysis) plot conducted on the normalized gene expression values of the samples. X- and Y-axes show the PC1 and PC2, respectively, with the amount of variance explained by each component reported in parenthesis. Blue dots in the plot represent replicates of control and red dots are rosiglitazone treated samples. (A) PCA plot of all 6 samples. (B) A new PCA plot generated after excluding 1 outlier.
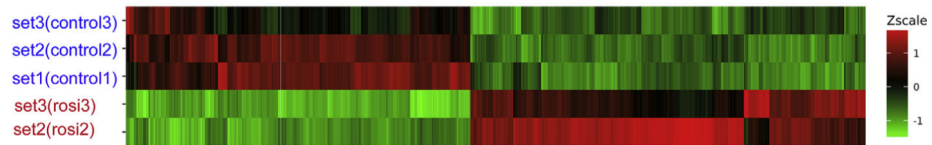
Fig. 2.
Heat map showing expression patterns (Z-scaled RPKM values) of the differentially expressed gens (DEG) from DESeq2 analysis. Changes in expression levels are displayed from green (less expressed) to red (more expressed). The order of the genes was established after hierachial clustering using the Euclidean distance.
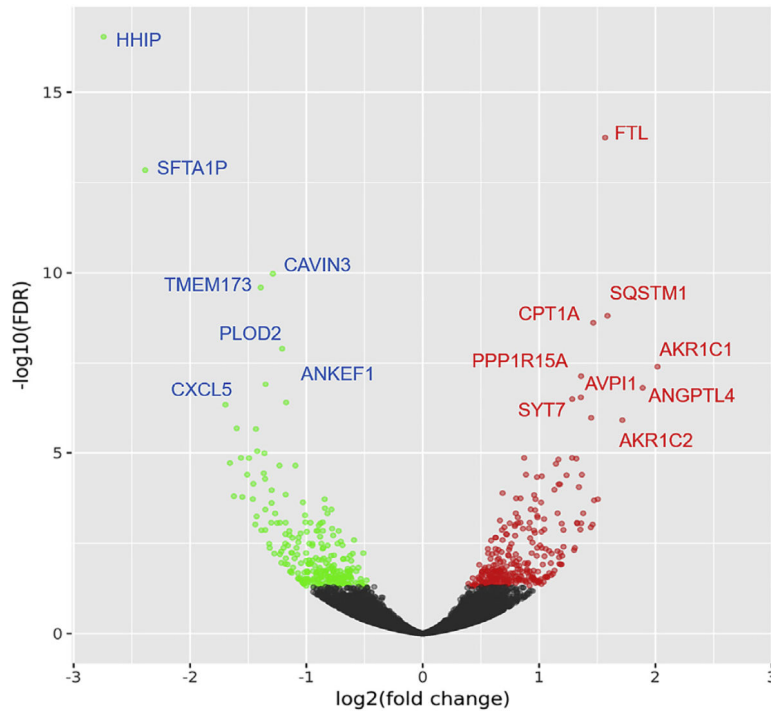
Fig. 3.
The Volcano plot showing the relationship between the fold-change (on the X-axis) and the significance of the differential expression test (Y-axis) for each gene from DESeq2 analysis. Black dots represent the genes that are not significantly differentially expressed, while red and green dots are the genes that are significantly up- and down-regulated, respectively. FTL: Ferritin light chain, SQSTM1: Sequestosome-1, CPT1A: Carnitine palmitoyltransferase 1A, AKR1C1: Aldo-ketoreductase family 1 member C1, PPP1R15A: Protein phosphatase 1 regulatory subunit 15A, ANGPTL4: Angiopoietin-related protein 4, AVPI1: Arginine vasopressin-induced protein 1, SYT7: Synamptotagmin-7, AKR1C2: Aldo-ketoreductase family 1 member C2. HHIP: Hedgehog-interacting protein, SFTA1P: Surfactant associated 1 pseudogene, CAVIN3: Protein kinase C delta-binding protein, TMEM173: Stimulator of interferon genes protein, PLOD2: Procollagen-lysin 2-oxoglutarate 5-dioxygenase 2, CXCL5: C-X-C motif chemokine 5, ANKEF1: Ankyrin-repeat and EF hand-domain containing protein 1.

PANTHER GO-Slim Biological Process
Total # Genes: 290   Total # process hits: 488

PANTHER GO-Slim Biological Process
Total # Genes: 298   Total # process hits: 405

- biological adhesion (GO:0022610)
- biological regulation (GO:0065007)
- cellular component organization or biogenesis (GO:0071840)
- cellular process (GO:0009987)
- developmental process (GO:0032502)
- immune system process (GO:0002376)
- localization (GO:0051179)
- locomotion (GO:0040011)
- metabolic process (GO:0008152)
- multicellular organismal process (GO:0032501)
- reproduction (GO:0000003)
- response to stimulus (GO:0050896)
- rhythmic process (GO:0048511)

PANTHER GO-Slim Biological Process
Level 1: metabolic process (GO:0008152)
Total # Genes: 97   Total # process hits: 203

PANTHER GO-Slim Biological Process
Level 1: metabolic process (GO:0008152)
Total # Genes: 91   Total # process hits: 200

- biosynthetic process (GO:0009058)
- catabolic process (GO:0009056)
- coenzyme metabolic process (GO:0006732)
- generation of precursor metabolites and energy (GO:0006091)
- nitrogen compound metabolic process (GO:0006807)
- phosphate-containing compound metabolic process (GO:0006796)
- primary metabolic process (GO:0044238)
- sulfur compound metabolic process (GO:0006790)
- vitamin metabolic process (GO:0006766)

PANTHER GO-Slim Biological Process
Level 1: cellular process (GO:0009987)
Total # Genes: 136   Total # process hits: 73

PANTHER GO-Slim Biological Process
Level 1: cellular process (GO:0009987)
Total # Genes: 124   Total # process hits: 64

- cell communication (GO:0007154)
- cell cycle (GO:0007049)
- cell growth (GO:0016049)
- cell proliferation (GO:0008283)
- cell recognition (GO:0008037)
- cellular component movement (GO:0006928)
- chromosome segregation (GO:0007059)
- cytokinesis (GO:0000910)
- viral process (GO:0016032)

Fig. 4.

Gene Ontology (GO) analysis of differentially expressed genes identified from NOISeq analysis. (A) Biological process of upregulated set (left) and downregulated set (right). GO analysis shows that the biological processes affected mostly by rosiglitazone are cellular and metabolic processes. (B) Level 1 metabolic process shows that primary metabolic process and biosynthetic process are highly represented both in upregulated (left) and downregulated set (right). (C) Level 1 cellular process shows that genes involved in cell communication and cell cycle are highly represented both in upregulated (left) and downregulated set (right).
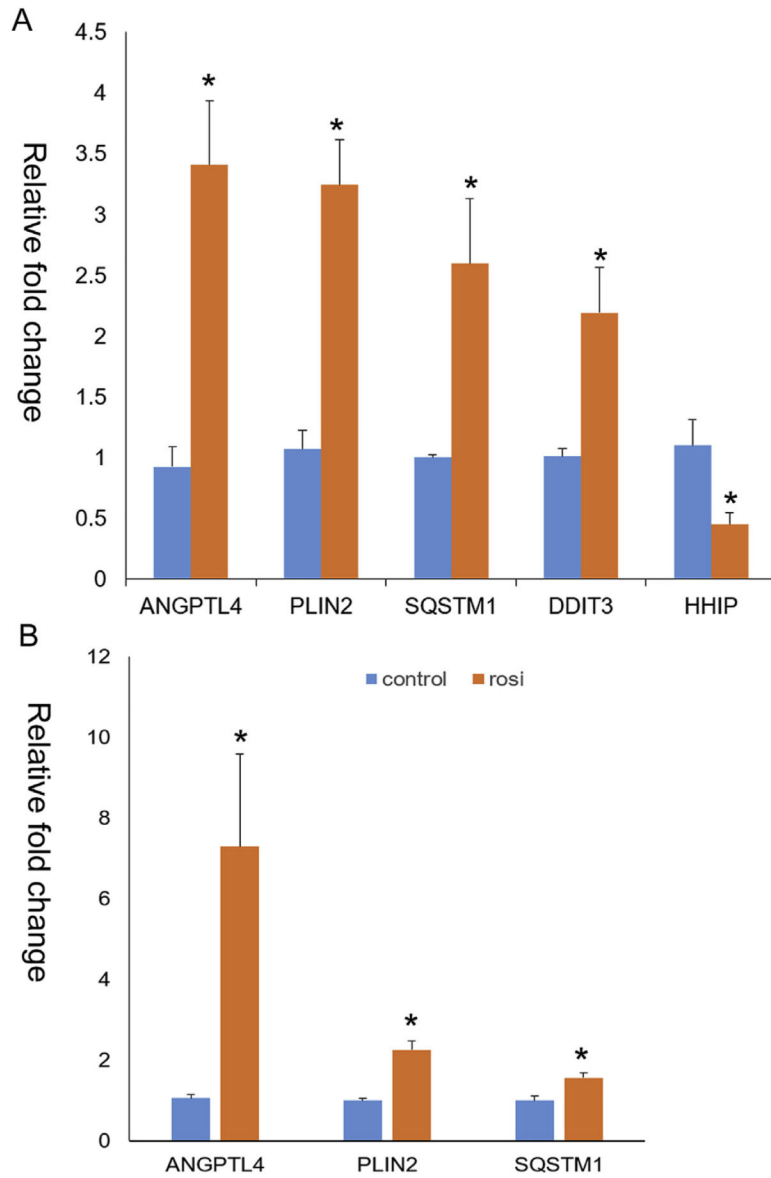
Fig. 5.
Quantitative PCR of ANGPTL4, PLIN2, SQSTM1, DDIT3, and HHIP. (A) Rosiglitazone 24 h after treatment significantly upregulated expression of ANGPTL4, PLIN2, SQSTM1, and DDIT3 by 3.4, 3.2, 2.6, and 2.2 folds on average, relatively. HHIP was downregulated after treatment with rosiglitazone by 2.2 fold. (B) Upregulated expression of ANGPTL4, PLIN2, and SQSTM1 after 6 days of rosiglitazone treatment (*: $P < 0.05$).
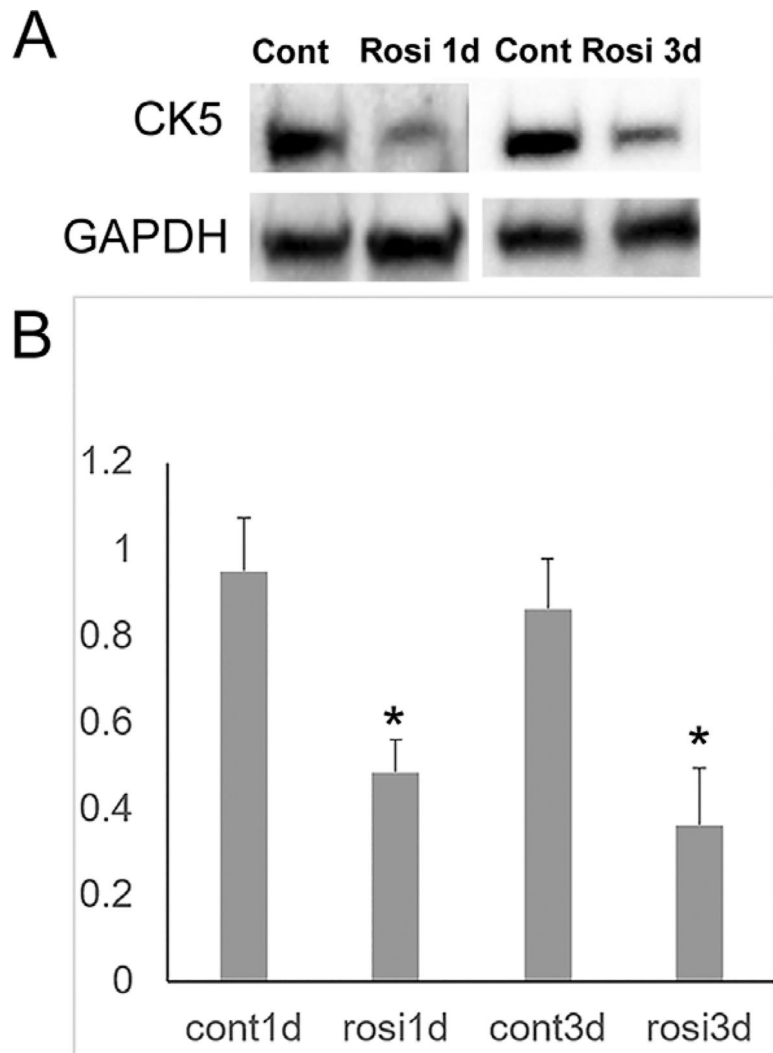
Fig. 6.
Western blot of CK5. (A) Representative image showing downregulation of CK5 in cells treated with rosiglitazone. (B) Bar graph obtained from 4 independent experiments. Rosiglitazone significantly downregulated expression of CK5 in hMGECs after both 1d and 3d treatment (*: $P < 0.05$).

Table 1

Gene Ontologies of upregulated genes by rosiglitazone in hMGEC.

GO_ID	GO_ biological process description	Item	P_value	FDR	E_Score
GO:0030968	endoplasmic reticulum unfolded protein response	9	1.95E-09	3.52E-08	12.63
GO:0034976	response to endoplasmic reticulum stress	7	1.97E-05	2.88E-04	6.10
GO:0045766	positive regulation of angiogenesis	8	2.37E-05	3.38E-04	5.23
GO:0042787	protein ubiquitination involved in ubiquitin-dependent protein catabolic process	9	1.43E-05	2.12E-04	4.98
GO:0006461	protein complex assembly	7	3.55E-04	2.53E-03	4.05
GO:0018105	peptidyl-serine phosphorylation	8	1.75E-04	1.37E-03	4.04
GO:0030308	negative regulation of cell growth	7	4.56E-04	2.83E-03	3.90
GO:0001525	Angiogenesis	12	2.05E-05	2.97E-04	3.77
GO:0043161	proteasome-mediated ubiquitin-dependent protein catabolic process	11	5.18E-05	6.94E-04	3.67
GO:0000165	MAPK cascade	14	1.94E-05	2.85E-04	3.39
GO:0046777	protein autophosphorylation	8	6.68E-04	3.52E-03	3.37
GO:0016569	covalent chromatin modification	13	7.46E-05	9.74E-04	3.16
GO:0006468	protein phosphorylation	25	5.38E-07	9.03E-06	2.92
GO:0016310	Phosphorylation	28	1.33E-07	2.30E-06	2.92
GO:0043065	positive regulation of apoptotic process	13	2.77E-04	2.06E-03	2.78
GO:0035556	intracellular signal transduction	17	7.17E-05	9.45E-04	2.70
GO:0010628	positive regulation of gene expression	13	5.07E-04	2.83E-03	2.62
GO:0000122	negative regulation of transcription from RNA polymerase II promoter	24	4.64E-05	6.26E-04	2.32
GO:0016567	protein ubiquitination	18	3.61E-04	2.57E-03	2.30
GO:0006629	lipid metabolic process	17	6.09E-04	3.25E-03	2.26
GO:0043066	negative regulation of apoptotic process	17	6.47E-04	3.43E-03	2.25
GO:0055114	oxidation-reduction process	21	7.64E-04	3.93E-03	2.03

Table 2

Gene Ontologies of downregulated genes by rosiglitazone in hMGEC.

GO_ID	GO_Description	Item	P_value	FDR	E_Score
GO:0097194	execution phase of apoptosis	6	2.07E-07	4.35E-06	13.94
GO:0006270	DNA replication initiation	5	2.50E-06	5.08E-05	12.59
GO:0031124	mRNA 3-end processing	5	6.21E-05	1.00E-03	7.31
GO:0032092	positive regulation of protein binding	5	8.12E-05	1.12E-03	6.97
GO:0006369	termination of RNA polymerase II transcription	5	1.81E-04	1.62E-03	6.04
GO:0000082	G1/S transition of mitotic cell cycle	6	1.38E-04	1.27E-03	5.33
GO:0032355	response to estradiol	5	8.96E-04	4.39E-03	4.49
GO:0010033	response to organic substance	5	1.04E-03	4.98E-03	4.36
GO:0006260	DNA replication	8	1.03E-04	1.12E-03	4.34
GO:0051607	defense response to virus	8	1.74E-04	1.57E-03	4.05
GO:0001666	response to hypoxia	8	2.41E-04	2.12E-03	3.88
GO:0032496	response to lipopolysaccharide	8	3.95E-04	2.55E-03	3.63
GO:0043123	positive regulation of I-KB kinase/NF KB signaling	7	7.74E-04	3.92E-03	3.60
GO:0000398	mRNA splicing, via spliceosome	9	9.77E-04	4.67E-03	2.98
GO:0006281	DNA repair	12	4.74E-04	2.95E-03	2.75
GO:0006397	mRNA processing	12	5.45E-04	3.35E-03	2.71
GO:0008380	RNA splicing	9	2.92E-03	9.59E-03	2.57

Table 3

Selected sets of differentially expressed genes by rosiglitazone in hMGEC.

Gene ID	FDR	P-value	logFC	Present in	Alias	Description
ENSG00000167772	1.57E-07	1.59E-10	1.89	D, E, R, N	ANGPTL4	Angiopoietin-related protein 4
ENSG00000147872	4.87E-03	6.81E-05	1.30	D, R, N	PLIN2	Perilipin-2
ENSG00000161011	1.54E-09	7.78E-13	1.59	D, E, R, N	SQSTM1	Sequestosome-1
ENSG00000181652	1.10E-16	NA	1.65	N	ATG9B	Autophagy-related protein 9B
ENSG00000175197	7.74E-03	1.26E-04	1.17	D, R, N	DDIT3	DNA damage-inducible transcript 3 protein
ENSG00000135218	1.07E-02	NA	1.41	N	CD36	Fatty acid translocase
ENSG00000164181	6.67E-16	NA	1.16	N	ELOVL7	Elongation of very long chain fatty acids protein 7
ENSG00000118402	0	NA	1.00	N	ELOVL4	Elongation of very long chain fatty acids protein 4
ENSG00000245848	2.80E-3	NA	1.70	N	CEBPA	CCAAT/enhancer-binding protein alpha
ENSG00000185950	3.0 E-3	1.1 E-3	0.94	D,E,N	IRS2	Insulin receptor substrate 2
ENSG00000164161	2.89E-17	2.43E-21	−2.74	D,E,R,N	HHIP	Hedgehog-interacting protein
ENSG00000175305	1.38E-3	1.27E-5	−1.39	D,E,R,N	CCNE2	Cyclin E2
ENSG00000186081	6.76E-3	1.06E-4	−0.76	D,E,N	CK5	Keratin II cytoskeletal 5
ENSG00000132646	2.39 E−2	6.74E-4	−0.87	D.N	PCNA	Proliferating cell nuclear antigen

D: DESeq2, E:EBSeq, R: edgeR, N: NOISeq.